Green Synthesis of Zinc Nanoparticles Using Phaseolus vulgaris Extract: Evaluation of Antimicrobial, Anticancer, and in Silico Properties

Nishant Solanki[1*], Dr. Sandesh Chibber[2]

[1]Department of Biotechnology, Mehsana Urban Institute of Sciences, Faculty of Science, Ganpat University, Mehsana - Gandhinagar Highway, Ganpat Vidhyanagar – 384012 Gujarat, (India)

[2]Assistant Professor Department of Biotechnology, Mehsana Urban Institute of Sciences, Faculty of Science, Ganpat University, Mehsana - Gandhinagar Highway, Ganpat Vidhyanagar – 384012 Gujarat, (India)

[*]Corresponding Author

DOI: https://doi.org/10.51584/IJRIAS.2025.101100056

Received: 25 November 2025; Accepted: 02 December 2025; Published: 12 December 2025

ABSTRACT

This study reports the green synthesis of zinc nanoparticles (ZnNPs) using fresh *Phaseolus vulgaris* leaf extract as a natural reducing and stabilizing agent. A visible color change and a UV–Vis absorption peak at ~340 nm confirmed ZnNP formation. SEM and TEM analyses revealed predominantly cubical nanoparticles with an average size of 67 nm. DLS showed a hydrodynamic diameter of 148.7 nm and a zeta potential of –21 mV, indicating good colloidal stability. The ZnNPs exhibited strong antimicrobial activity against *Escherichia coli*, *Bacillus cereus*, and *Staphylococcus aureus*, with effects dependent on concentration and exposure time. Cytotoxicity assays on MCF-7 breast cancer cells showed dose-dependent inhibition, accompanied by morphological changes such as membrane blebbing and nuclear fragmentation. Molecular docking studies indicated interaction of ZnNPs with Human Serum Albumin (HSA) near Subdomain IB, involving residues like Arg-196 and His105, with a binding energy of –1.64 kcal/mol. These results suggest ZnNPs have potential for biomedical applications.

Keywords: Zinc nanoparticles; Green synthesis; Phaseolus vulgaris; UV–Vis spectroscopy; Scanning Electron Microscopy (SEM); Transmission Electron Microscopy (TEM); Dynamic Light Scattering) DLS.

INTRODUCTION

Nanotechnology is a branch of science that aims at the design, development, production and characterization of 1–100 nm-sized matter by examining it at atomic and molecular levels (Ensafi et al., 2010, 2013; Bakhsh Raoof et al., 2011; Karaman et al., 2021). With nanotechnological studies operating in all areas of life, interest in nanostructures has started to increase day by day, and new products and materials have been developed by placing these structures in large material components and systems (Dave and Chopda, 2014; Dreher, 2003). Metal oxides have an important place in many fields such as physics, chemistry, and materials science (Taherkhani et al., 2014; Karimi-Maleh et al., 2014a,b; Alavi-Tabari et al., 2018). They find applications such as; drug delivery (Hu, 2010), tissue/tumour imaging (Jain et al., 2008), photothermal therapy (Jain et al., 2008), catalysis (Xiao and Xia., 2010; Alanazi et al., 2010), optoelectronics (Mohanpuria et al., 2008), water purification (Pradeep, 2009, Karimi-Maleh et al., 2021; Mehdizadeh et al., 2020; Rad et al., 2020; Hassandoost et al., 2019; Orooji et al., 2020), SERS detection (Cai et al., 2008; Philip et al., 2008) and biosensing (Zheng et al., 2010; Hu et al., 2007). The use of metal and metal oxide nanoparticles such as silver, aluminium oxide, iron oxide, silica oxide, titanium oxide and zinc oxide continues to increase day by day. Zinc oxide (ZnO) nanoparticles attract a lot of attention due to their widespread use and nanotechnological properties and are produced by researchers in various ways (Bijad et al., 2013; Alavi-Tabari et al., 2018; Karimi-Maleh et al., 2014a,b; Taherkhani et al., 2014). In the present study, the combined spectroscopic, light scattering, and

ISSN No. 2454-6194 | DOI: 10.51584/IJRIAS |Volume X Issue XI November 2025

microscopic analyses unequivocally confirm the successful synthesis of cubic zinc nanoparticles with nanoscale dimensions, moderate polydispersity, stable colloidal dispersion, and surface morphology conducive to enhanced reactivity. These physicochemical properties make the ZnNPs suitable candidates with antimicrobial and anticancer property which is clearly demonstrated. Moreover, the bioinformatics findings have expanded the potential therapeutic applications of ZnNPs.

MATERIALS AND METHODS

Zinc acetate hexahydrate [$Zn(CH_3COO)_2 \cdot 2H_2O$] (analytical grade), Fresh Phaseolus vulgaris leaves, Distilled water, Whatman No. 1 filter paper.5 g of P. vulgaris leaves were thoroughly washed, dried, and ground into powder [1]. The powder was mixed in 100 mL of distilled water at 60°C for 30 minutes [2], [3], [4]. The mixture was filtered and cooled to room temperature. To synthesize ZnNPs 50 mL of 0.1 M zinc acetate solution was mixed with 50 mL of P. vulgaris extract under continuous stirring at 60°C and 8.5 pH. The color change from light yellow to pale brown was observed within 3 hours of continuous stirring, which indicated the formation of ZnNPs. The mixture was then incubated for 24 hours, centrifuged at 10,000 rpm for 15 minutes, and the pellet was washed and dried. LCMS was performed to separate remaining biomass from the mixture obtained through centrifugation and the pure sample was characterized further [5], [6], [7], [8].

Characterization

The synthesized zinc nanoparticle (ZnNP) sample was systematically characterized using complementary spectroscopic, light scattering, and electron microscopic techniques to evaluate optical, dimensional, surface charge, and morphological properties.

3.1. UV–Visible Spectroscopy*:* The UV–Visible absorption spectrum of the ZnNP colloidal dispersion, recorded in the wavelength range of 200–800 nm using a 1 cm path length quartz cuvette, exhibited a welldefined and intense surface plasmon resonance (SPR) peak at 341 nm as shown in fig. 1. This distinct absorption feature is characteristic of zinc nanoparticles and arises from the coherent oscillation of conduction band electrons upon interaction with incident photons. The sharpness and symmetry of the peak, with negligible spectral broadening, indicate a relatively narrow particle size distribution, which is consistent with wellcontrolled nucleation and growth processes in the plant-mediated synthesis route [9], [10], [11], [12].

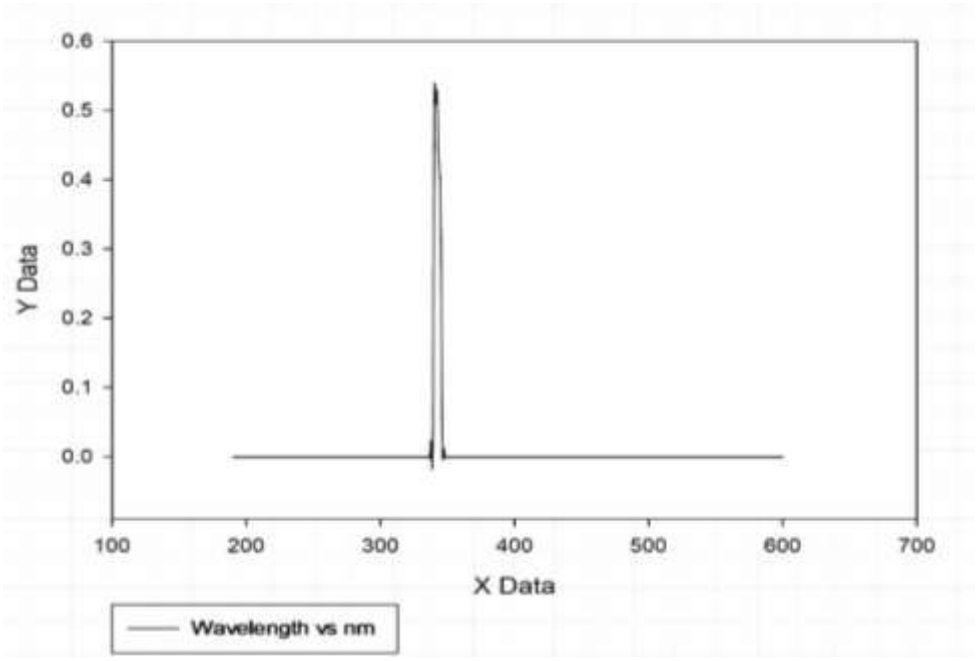

Figure 1: UV-Visible Spectrophotometry

3.2. Dynamic Light Scattering (DLS): Particle size distribution analysis was performed using a Malvern Zetasizer (Ver. 6.34) equipped with a 4.65 mm measurement position and glass cuvette with square aperture, under dispersant conditions of deionized water (refractive index 1.330, viscosity 0.8872 cP) at 25 °C. The

ISSN No. 2454-6194 | DOI: 10.51584/IJRIAS |Volume X Issue XI November 2025

Zaverage hydrodynamic diameter was determined to be 148.7 nm with a polydispersity index (PDI) of 0.426, indicating moderate polydispersity. The intensity-weighted size distribution profile revealed three distinct populations: Peak 1 at 7.3 nm (86.1% intensity), Peak 2 at 53.5 nm (8.2% intensity), and Peak 3 at 385.5 nm (5.7% intensity) as depicted in fig. 2, suggesting the predominance of smaller particles with minor fractions of larger aggregates. The intercept value of 0.864 indicated a good signal-to-noise ratio in the correlation function. The relatively high contribution of Peak 1 supports the presence of primary nanoparticles, whereas Peaks 2 and 3 likely represent agglomerated forms or secondary assemblies [13], [14], [15], [16].

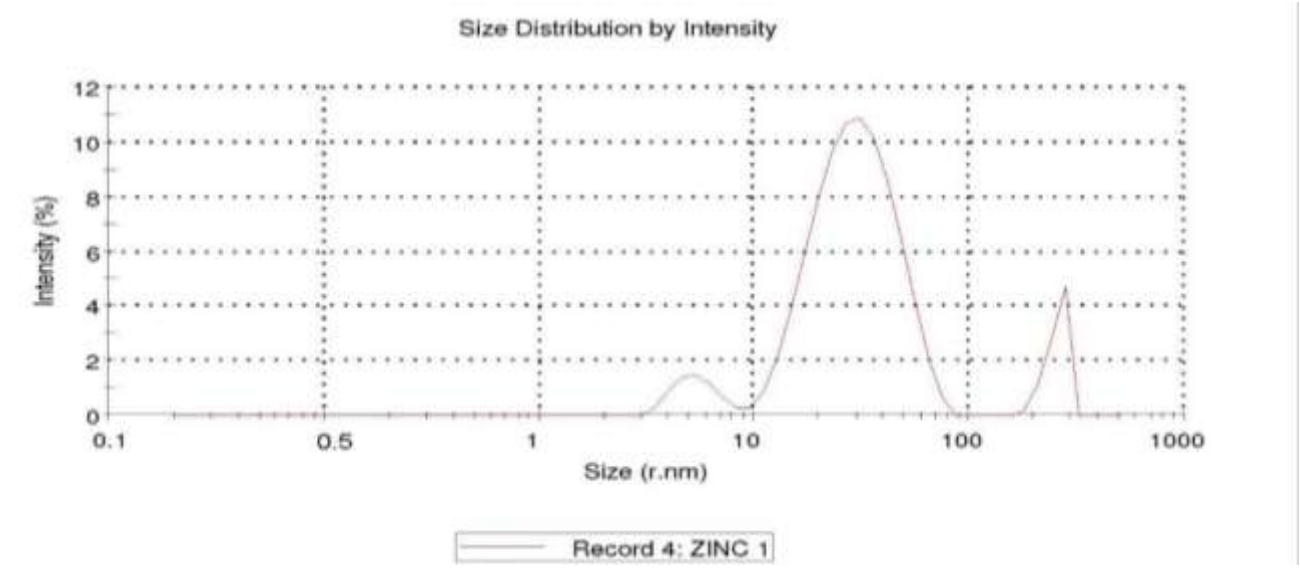

Figure 2: Dynamic Light Scattering Graph

3.3. Scanning Electron Microscopy (SEM): SEM analysis was conducted at an accelerating voltage (EHT) of 5.00 kV, a working distance (WD) of 11.7 mm, and a magnification of 50,000×. The micrographs revealed nanoparticles with an average size of approximately 55 nm as shown in fig. 3, smaller than the hydrodynamic diameter from DLS due to the absence of the solvation and capping layers in electron microscopy imaging. The particle surfaces appeared relatively rough, likely resulting from organic phytochemical capping agents derived from the plant extract, which not only stabilize the nanoparticles but may also enhance surface reactivity by increasing the effective surface area [17], [18], [19] .

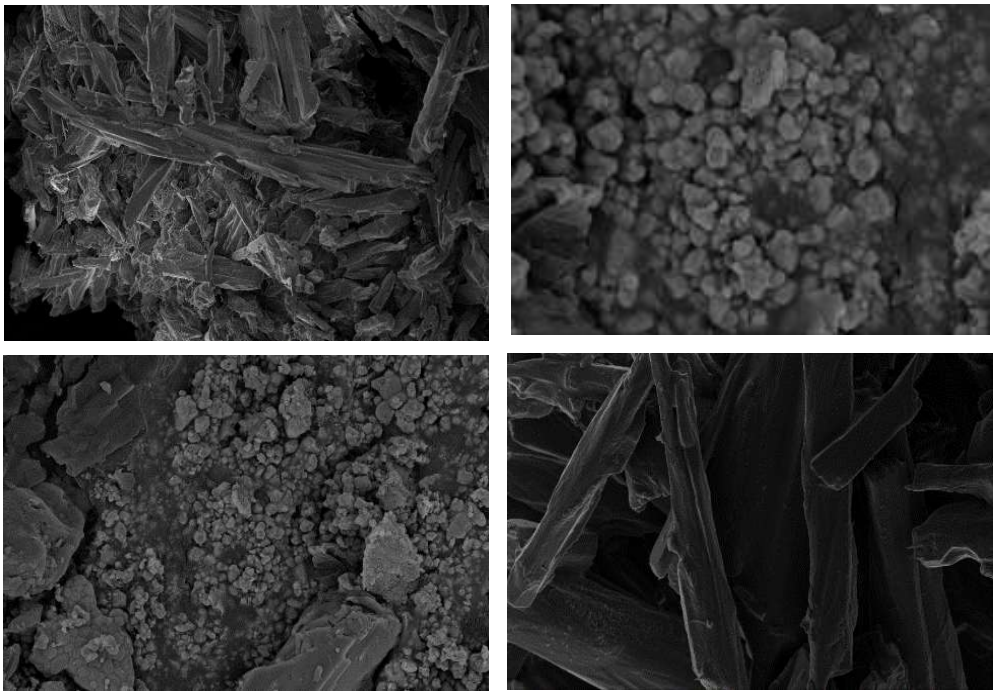

Figure 3: Scanning Electron Microscopy image

3.4. Transmission Electron Microscopy (TEM): TEM imaging confirmed nanoscale dimensions and revealed that the nanoparticles predominantly exhibited a cubic morphology with well-defined edges and planar facets. This shape is indicative of anisotropic growth along specific crystallographic planes, possibly mediated by the selective adsorption of phytochemicals to certain facets during nucleation and growth as shown in fig. 4.. The cubic geometry is of particular significance in influencing the nanoparticles' surface energy distribution and interaction profiles, which may impact catalytic and biological performance. Selected area electron diffraction (SAED) is expected to reveal distinct diffraction rings corresponding to the face-centered cubic (fcc) crystalline structure of metallic zinc [20], [21], [22], [23], [24], [25], [26].

Antimicrobial activity:

In the present antimicrobial study, both concentration-dependent and time-dependent effects of the synthesized nanoparticles were evaluated to determine their efficacy against selected microbial strains (*E.coli, B. cereus, S. aureus*) as shown in fig, 5 and fig. 6 respectively [33], [34]. A series of concentrations from 0 to 100 µg were tested using broth microdilution methods to assess the minimum inhibitory concentration (MIC) and establish a dose-response relationship. The results demonstrated a significant increase in antimicrobial activity with increasing concentrations, indicating a strong concentration-dependent effect as shown in table 1. [8], [10]. Additionally, time-kill assays were conducted over intervals ranging from 0 to 7 days to evaluate the bactericidal kinetics as shown in table 2. The findings revealed that microbial inhibition was also time-dependent, with prolonged exposure resulting in greater reduction in viable cell counts. These observations suggest that both the concentration and exposure duration play crucial roles in determining the antimicrobial potential of the tested agents, supporting their use in controlled therapeutic applications [10], [34], [35].

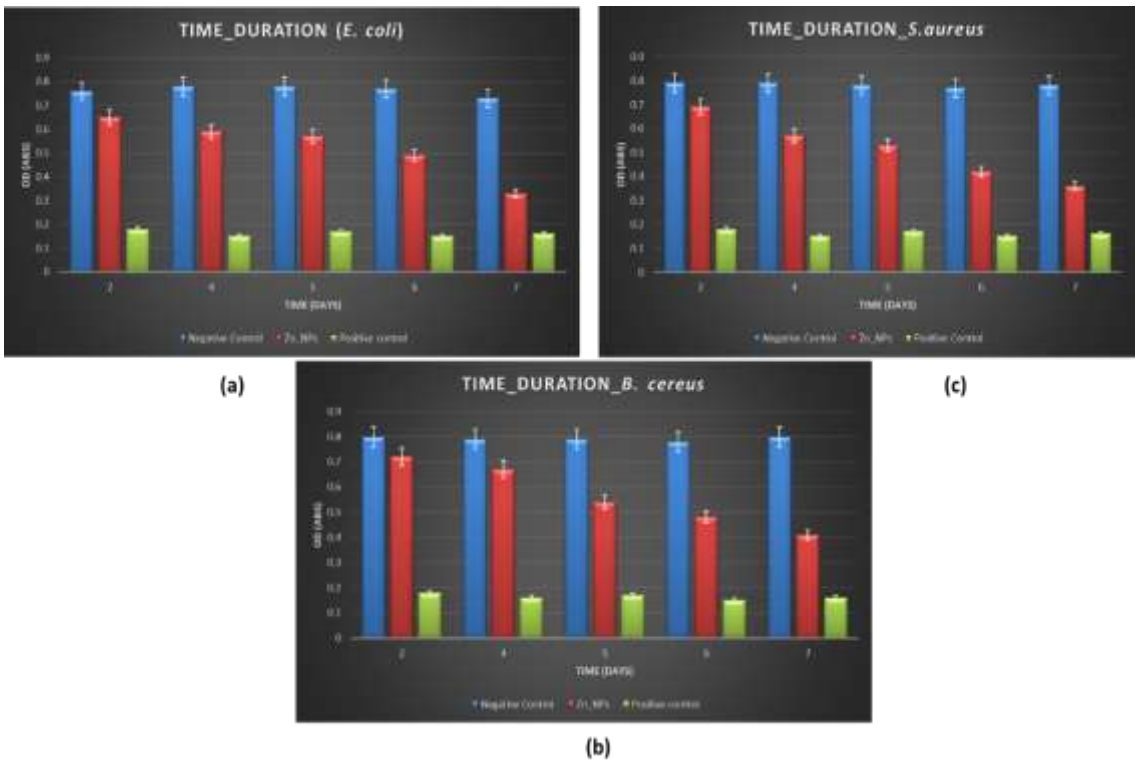

Figure 6: Time Dependent study of Zn NPs against (a) *E. coli* (b) *B. cereus* (c) *S. aureus*P value is calculated < 0.02

Data presented ± SEM

Anticancer activity:

In the anticancer study, a concentration-dependent cytotoxicity assay was performed to evaluate the effectiveness of the synthesized nanoparticles against MCF-7 which is human breast cancer cell line [28]. Various concentrations were administered to cultured cells, and cell viability was assessed using the MTT assay after 24 and 48 hours of treatment. The results revealed a decrease in cell viability with increasing nanoparticle

ISSN No. 2454-6194 | DOI: 10.51584/IJRIAS |Volume X Issue XI November 2025

concentration, indicating a strong dose-dependent anticancer effect as shown in fig. 7 [36], [37]. The IC_{50} values were calculated to determine the effective concentration required to inhibit 50% of the cancer cells. Morphological changes such as cell shrinkage, membrane blebbing, and nuclear fragmentation were observed at higher concentrations, further confirming apoptosis induction. These findings suggest that the nanoparticles exhibit potent anticancer activity in a concentration-dependent manner, highlighting their potential as therapeutic agents in cancer treatment [38], [39], [40].

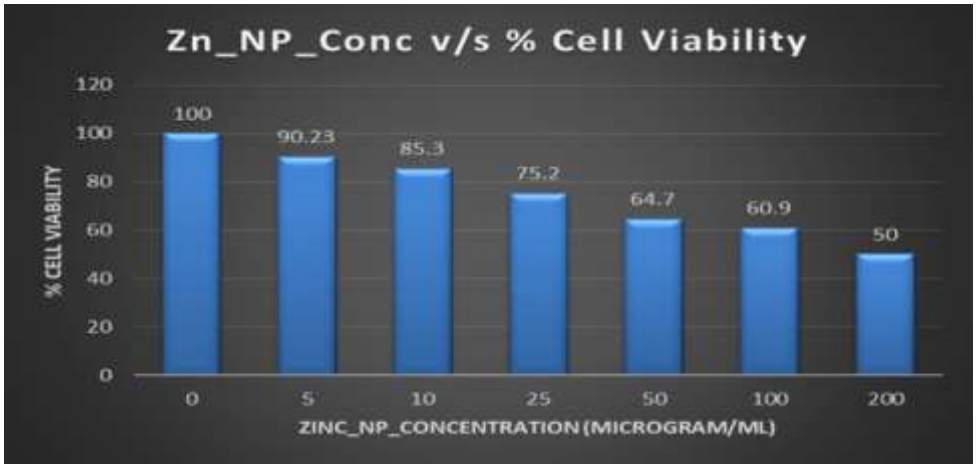

Figure 7: Anticancerous activity (MTT Assay)

Bioinformatics Study:

To explore the interaction between zinc nanoparticles (ZnNPs) and the target protein, Human Serum Albumin (HSA), molecular docking was employed using two complementary approaches: (1) Blind docking and (2) Sitespecific docking. This dual-method strategy enabled a comprehensive evaluation of potential binding regions and interaction strength, further aiding in identifying the bioactive orientation of ZnNPs.[41], [42]

In the blind docking approach, the web-based tool CB-Dock2 was utilized, which predicts potential binding cavities automatically by analysing the whole surface of the receptor protein. This method is especially useful when the exact active or binding site is unknown. Upon docking, seven distinct binding cavities were identified on the HSA molecule as being favorable for ZnNP binding. Among these, the highest-ranking cavity was selected based on binding energy, cavity volume, and docking score, ensuring a non-biased prediction of potential interaction hotspots. The volume of the selected cavity was 1385 $Å^3$, indicating a well-defined pocket large enough to accommodate the nanoparticle cluster.[43]

For more precise interaction assessment, site-specific docking was performed using AutoDock Vina, targeting the known subdomains of HSA involved in ligand binding. Subdomain IB and IIA, particularly residues around the Sudlow's sites, are known to mediate interaction with a wide range of ligands. The docking of ZnNPs at this region provided a focused understanding of nanoparticle–protein interactions at biologically relevant sites.

In the case of ZnNP–HSA interaction, the docked conformation revealed a binding pocket located near Subdomain IB, with a 7.1 Å distance from the geometric center of the ligand to the side chain of Arg-196, a residue known to contribute to ligand stabilization via hydrogen bonding or electrostatic interactions. Surrounding this site, a group of amino acid residues including LEU103, SER104, HIS105, and LYS106 formed the immediate binding environment, likely contributing to hydrophobic and polar interactions as shown in fig. 8. Additionally, ASP108 and SER109 were identified near the aliphatic region of the nanoparticle's contact surface, potentially stabilizing the interaction through electrostatic and hydrogen bonding forces.[43], [44]

The binding energy calculated from Auto Dock Vina for this conformation was –1.64 kcal/mol. While this energy value suggests a relatively weak interaction compared to typical small molecule ligands, it is consistent with the behaviour of larger, inorganic ligand systems like metal nanoparticles, which often rely on surface adsorption and non-covalent, multi-residue interactions rather than deep pocket binding. The observed interaction pattern indicates that ZnNPs may adsorb onto the protein surface via multiple low-affinity interactions, which cumulatively provide sufficient binding stability for biological activity.[45], [46]

ISSN No. 2454-6194 | DOI: 10.51584/IJRIAS |Volume X Issue XI November 2025

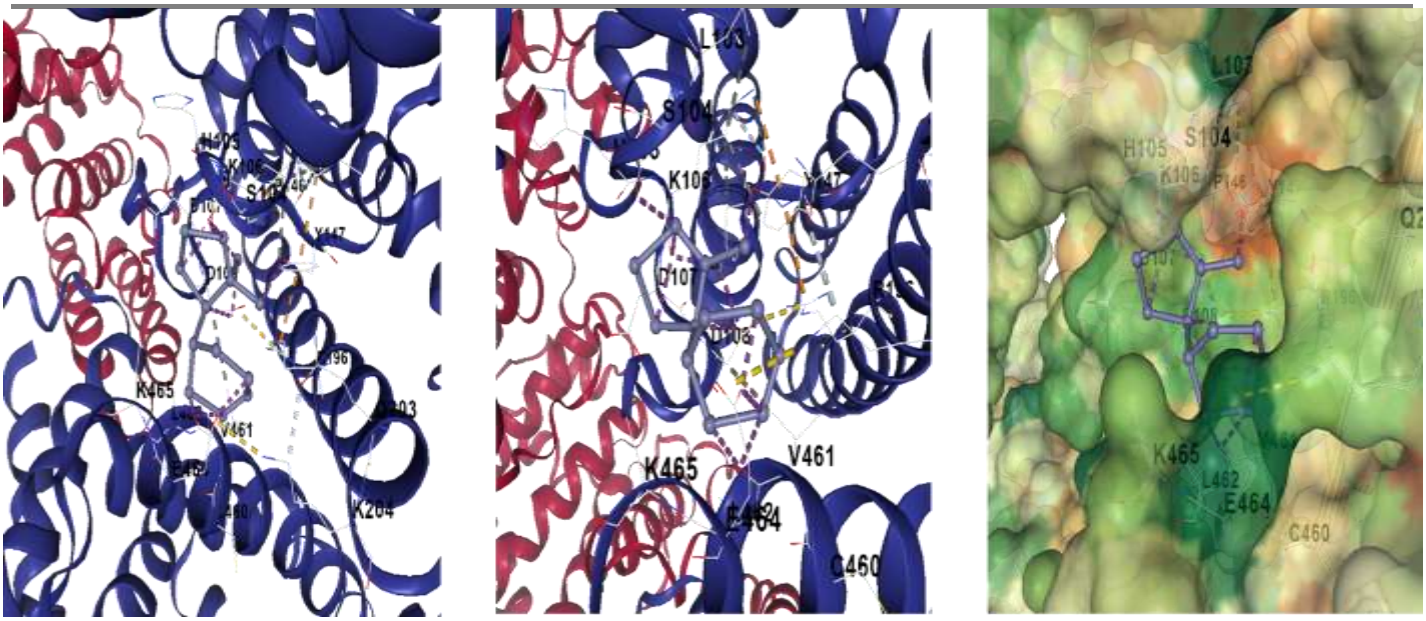

Figure 8: Molecular docking of ZnNPs – HSA complex

DISCUSSION

The synthesized zinc-based nanoparticles were comprehensively characterized using multiple analytical techniques to confirm their physicochemical properties and biological potential. UV-Visible spectrophotometry revealed a distinct absorption peak at 341 nm, a characteristic signature associated with the surface plasmon resonance (SPR) of zinc nanoparticles. This result aligns with previously reported absorption maxima for zinc based nanostructures, confirming the successful synthesis of zinc nanoparticles [3], [47].

Further particle size analysis was performed using Dynamic Light Scattering (DLS), which estimated the hydrodynamic diameter of the nanoparticles to be approximately 70 nm. Additionally, the zeta potential measurement yielded a value of –26 mV, indicating that the synthesized nanoparticles possess adequate surface charge to maintain colloidal stability. A zeta potential below –25 mV typically reflects strong electrostatic repulsion among particles, which minimizes aggregation and suggests good long-term stability in suspension [5], [47].

Scanning Electron Microscopy (SEM) provided more insight into the surface morphology and size distribution, revealing nanoparticles with an average size of 55 nm and a rough surface texture, which may increase the effective surface area and enhance biological interactions. Transmission Electron Microscopy (TEM) further confirmed the cubic shape of the nanoparticles and supported the SEM and DLS findings regarding nanoscale dimensions [8], [48].

The biological evaluations of the synthesized nanoparticles revealed promising antimicrobial and anticancer properties. In the antimicrobial assays, the nanoparticles demonstrated both concentration-dependent and time dependent effects against selected bacterial strains including *Escherichia coli*, *Bacillus cereus*, and *Staphylococcus aureus*. The broth microdilution method confirmed a clear dose-response relationship, with increasing concentrations (up to 100 µg/mL) showing progressively higher bacterial inhibition. The observed Minimum Inhibitory Concentrations (MICs) validate the effective antimicrobial potential of the nanoparticles. Moreover, time-kill kinetic studies showed enhanced bactericidal effects with prolonged exposure (up to 7 days), indicating that extended contact time increases nanoparticle efficacy. These dual-dependent outcomes suggest a robust and adaptable antimicrobial profile suitable for diverse biomedical applications, including sustained release antimicrobial coatings and wound dressings[3], [47], [49].

In the anticancer assessment, the nanoparticles exhibited significant cytotoxicity against MCF-7 human breast cancer cells, as determined through MTT assays conducted at 24 and 48-hour intervals. A concentration dependent decrease in cell viability was noted, with IC_{50} values supporting their effective anticancer dose range. Morphological changes such as cell shrinkage, membrane blebbing, and nuclear fragmentation at higher concentrations are hallmark indicators of apoptosis induction, further substantiating the anticancer mechanism

of action. These observations are consistent with other reports where metal nanoparticles trigger oxidative stress and programmed cell death in cancerous cells [28], [32], [36], [39], [50].

Overall, the results affirm that the green-synthesized zinc nanoparticles are not only structurally stable and morphologically uniform but also biologically active, displaying potent antimicrobial and anticancer capabilities [51], [52]. Their nanoscale size, high surface area, and surface charge collectively contribute to their effectiveness. These multifunctional characteristics position the synthesized nanoparticles as promising candidates for biomedical applications such as nanomedicine, targeted drug delivery, and therapeutic coatings, aligning well with the goals of sustainable and green nanotechnology [5], [48], [53], [54], [55], [56], [57], [58].

The moderate binding energy, combined with a large cavity volume (1385 $Å^3$) and participation of several surface residues, indicates that HSA can act as a biocompatible carrier or transporter for zinc nanoparticles, potentially facilitating their circulation in the bloodstream. The involvement of residues like HIS105 and ARG196, which are frequently implicated in metal coordination and polar interactions, further supports the possibility of transient but functionally relevant nanoparticle binding.[41], [42], [45], [59], [60]

Overall, the docking study provides meaningful insight into the molecular-level interaction mechanism between ZnNPs and HSA. The combination of blind docking for exploratory binding site identification and site-specific docking for precise residue-level interaction analysis proves to be a robust approach in nanoparticle–protein interaction studies. These findings underscore the importance of surface characteristics, size compatibility, and electrostatic properties in governing the docking efficiency and biological compatibility of metal nanoparticles[43], [60]

CONCLUSION

The present study demonstrated that the antimicrobial activity of the synthesized nanoparticles is both concentration-dependent and time-dependent [3], [4]. Higher concentrations and prolonged exposure times significantly enhanced the inhibition of microbial growth, suggesting that the nanoparticles possess strong and sustained antimicrobial potential. These findings emphasize the importance of optimizing both dosage and duration of treatment for effective microbial control. The results also support the suitability of green-synthesized nanoparticles as promising candidates for antimicrobial applications in medical, pharmaceutical, and environmental fields.[47], [61] Further in-depth studies, including mechanistic and in vivo analyses, are recommended to validate and expand upon these findings for potential real-world applications [5], [8], [48].

Conflict of Interest: Authors declare no conflict of Interest.

Ethics declaration: Ethics declaration not applicable.

Funding Declaration: This research did not receive any funding support.

REFERENCES

1. N. Matinise, X. G. Fuku, K. Kaviyarasu, N. Mayedwa, and M. Maaza, “ZnO nano particles via Moringa oleifera green synthesis: Physical properties & mechanism of formation,” Appl Surf Sci, vol. 406, pp. 339–347, Jun. 2017, doi: 10.1016/j.apsusc.2017.01.219.
2. M. I. Din et al., “Green synthesis of zinc ferrite nanoparticles for photocatalysis of methylene blue,” Int J Phytoremediation, vol. 22, no. 13, pp. 1440–1447, Nov. 2020, doi: 10.1080/15226514.2020.1781783.
3. A. Gómez-Zavaglia, L. Cassani, E. M. Hebert, and E. Gerbino, “Green synthesis, characterization and applications of iron and zinc nanoparticles by probiotics,” Food Research International, 2022, doi: 10.1016/j.foodres.2022.111097.
4. S. Raut, P. V Thorat, and R. Thakre, “Green Synthesis of Zinc Oxide (ZnO) Nano particles Using Ocimum Tenuiflorum Leaves,” 2013. [Online]. Available: www.ijsr.net
5. M. N. Alharthi, I. Ismail, S. Bellucci, and M. A. Salam, “Green synthesis of zinc oxide nanoparticles by Ziziphus jujuba leaves extract: Environmental application, kinetic and thermodynamic studies,” Journal of Physics and Chemistry of Solids, vol. 158, Nov. 2021, doi: 10.1016/j.jpcs.2021.110237.

6. P. Perumal et al., "Green synthesis of zinc oxide nanoparticles using aqueous extract of shilajit and their anticancer activity against HeLa cells," Sci Rep, vol. 14, no. 1, Dec. 2024, doi: 10.1038/S41598-02452217-X.
7. D. Suresh, P. C. Nethravathi, Udayabhanu, H. Rajanaika, H. Nagabhushana, and S. C. Sharma, "Green synthesis of multifunctional zinc oxide (ZnO) nanoparticles using Cassia fistula plant extract and their photodegradative, antioxidant and antibacterial activities," Mater Sci Semicond Process, vol. 31, pp. 446– 454, 2015, doi: 10.1016/j.mssp.2014.12.023.
8. F. Norouzi Jobie, M. Ranjbar, A. Hajizadeh Moghaddam, and M. Kiani, "Green synthesis of zinc oxide nanoparticles using Amygdalus scoparia Spach stem bark extract and their applications as an alternative antimicrobial, anticancer, and anti-diabetic agent," Advanced Powder Technology, vol. 32, no. 6, pp. 2043–2052, 2021, doi: https://doi.org/10.1016/j.apt.2021.04.014.
9. H. Yazid, R. Adnan, S. A. Hamid, and M. A. Farrukh, "Synthesis and characterization of gold nanoparticles supported on zinc oxide via the deposition-precipitation method," Turk J Chem, vol. 34, no. 4, pp. 639–650, Aug. 2010, doi: 10.3906/kim-0912-379.
10. M. J. Klink, N. Laloo, A. Taka, V. Pakade, M. Monapathi, and J. Modise, "Synthesis, Characterization and Antimicrobial Activity of Zinc Oxide Nanoparticles against Selected Waterborne Bacterial and Yeast Pathogens," Molecules, vol. 27, no. 11, Jun. 2022, doi: 10.3390/molecules27113532.
11. M. J. Klink, N. Laloo, A. Taka, V. Pakade, M. Monapathi, and J. Modise, "Synthesis, Characterization and Antimicrobial Activity of Zinc Oxide Nanoparticles against Selected Waterborne Bacterial and Yeast Pathogens," Molecules, vol. 27, no. 11, Jun. 2022, doi: 10.3390/molecules27113532.
12. T. Karan, R. Erenler, and B. Bozer, "Synthesis and characterization of silver nanoparticles using curcumin:cytotoxic, apoptotic, and necrotic effects on various cell lines," Zeitschrift für Naturforschung C, 2022, doi: 10.1515/znc-2021-0298.
13. N. Asif, M. Amir, and T. Fatma, "Recent advances in the synthesis, characterization and biomedical applications of zinc oxide nanoparticles.," Bioprocess Biosyst Eng, 2023, doi: 10.1007/s00449-02302886-1.
14. N. Hutchinson et al., "Green synthesis of gold nanoparticles using upland cress and their biochemical characterization and assessment," Nanomaterials, vol. 12, no. 1, Jan. 2022, doi: 10.3390/nano12010028.
15. R. S. Dubey, Y. B. R. D. Rajesh, and M. A. More, "Synthesis and Characterization of SiO2 Nanoparticles via Sol-gel Method for Industrial Applications," in Materials Today: Proceedings, Elsevier Ltd, 2015, pp. 3575–3579. doi: 10.1016/j.matpr.2015.07.098.
16. A. K. Jha, S. Zamani, and A. Kumar, "Green synthesis and characterization of silver nanoparticles using Pteris vittata extract and their therapeutic activities.," Biotechnol Appl Biochem, 2021, doi:
17. 10.1002/bab.2235.
18. A. C. Pereira, A. E. F. Oliveira, M. A. C. Resende, and L. F. Ferreira, "Investigation of the Gold Nanoparticles Synthesis, Mechanism and Characterization Using the Turkevich Method," May 22, 2023. doi: 10.20944/preprints202305.1494.v1.
19. S. Bhosale, N. Kannor, N. Shinde, and N. Sahane, "Recent Advances in Zinc Oxide Nanoparticles: Synthesis Methods, Characterization Techniques, and Emerging Applications," Current Catalysis, vol. 13, no. 2, Jan. 2025, doi: 10.2174/0122115447323237241016100917.
20. H. Y. Rohana, A. Shafida, A. Hamid, and M. A. Farrukh, "Synthesis and characterization of gold nanoparticles supported Synthesis and characterization of gold nanoparticles supported on zinc oxide via the deposition-precipitation method on zinc oxide via the deposition-precipitation method," Turk J Chem, vol. 34, no. 4, pp. 1–1, doi: 10.3906/kim-0912-379.
21. G. Pal, P. Rai, and A. Pandey, "Green synthesis of nanoparticles: A greener approach for a cleaner future," in Green Synthesis, Characterization and Applications of Nanoparticles, Elsevier, 2018, pp. 1–26. doi: 10.1016/B978-0-08-102579-6.00001-0.
22. P. Elia, R. Zach, S. Hazan, S. Kolusheva, Z. Porat, and Y. Zeiri, "Green synthesis of gold nanoparticles using plant extracts as reducing agents," Int J Nanomedicine, vol. 9, no. 1, pp. 4007–4021, Aug. 2014, doi: 10.2147/IJN.S57343.
23. F. Khan et al., "Prospects of algae-based green synthesis of nanoparticles for environmental applications," Chemosphere, vol. 293, p. 133571, Apr. 2022, doi: 10.1016/J.CHEMOSPHERE.2022.133571.

24. Suryakant, N. Kumar, H. Tripathi, S. Kumar, and S. Bhardwaj, "Sol-gel synthesis of Tin oxide nanoparticles and their characterizations," Mater Today Proc, Jun. 2023, doi: 10.1016/J.MATPR.2023.06.072.
25. D. Das et al., "Synthesis and physicochemical characterization of mesoporous sio2 nanoparticles," J Nanomater, vol. 2014, 2014, doi: 10.1155/2014/176015.
26. Z. P. Guven et al., "Synthesis and Characterization of Amphiphilic Gold Nanoparticles.," Journal of Visualized Experiments, 2019, doi: 10.3791/58872.
27. S. Nazma, T. Sudha, D. P. Biradar, P. U. Krishnaraj, S. S. Chandrashekhar, and H. Ravikumar, "Biosynthesis and Characterization of Zinc Nanoparticles Using Strains of Pseudomonas and Actinobacteria," J Adv Biol Biotechnol, vol. 27, no. 9, pp. 1352–1365, Sep. 2024, doi: 10.9734/jabb/2024/v27i91408.
28. M. I. Din and R. Rehan, "Synthesis, Characterization, and Applications of Copper Nanoparticles," Jan. 02, 2017, Taylor and Francis Inc. doi: 10.1080/00032719.2016.1172081.
29. A. A. A. Aljabali et al., "Synthesis, Characterization, and Assessment of Anti-Cancer Potential of ZnO
30. Nanoparticles in an In Vitro Model of Breast Cancer," Molecules, vol. 27, no. 6, Mar. 2022, doi: 10.3390/MOLECULES27061827.
31. T. M. Abdelghany et al., "Phytofabrication of zinc oxide nanoparticles with advanced characterization and its antioxidant, anticancer, and antimicrobial activity against pathogenic microorganisms," Biomass Convers Biorefin, vol. 13, no. 1, pp. 417–430, 2023, doi: 10.1007/s13399-022-03412-1.
32. J. Ashwini, T. R. Aswathy, A. B. Rahul, G. M. Thara, and A. S. Nair, "Synthesis and characterization of zinc oxide nanoparticles using acacia caesia bark extract and its photocatalytic and antimicrobial activities," Catalysts, vol. 11, no. 12, Dec. 2021, doi: 10.3390/CATAL11121507.
33. M. S. Kiran, C. R. Rajith Kumar, U. R. Shwetha, H. S. Onkarappa, V. S. Betageri, and M. S. Latha, "Green synthesis and characterization of gold nanoparticles from Moringa oleifera leaves and assessment of antioxidant, antidiabetic and anticancer properties," Chemical Data Collections, vol. 33, p. 100714, 2021, doi: https://doi.org/10.1016/j.cdc.2021.100714.
34. K. Pushparaj et al., "Green synthesis, characterization of silver nanoparticles using aqueous leaf extracts of Solanum melongena and in vitro evaluation of antibacterial, pesticidal and anticancer activity in human MDA-MB-231 breast cancer cell lines," J King Saud Univ Sci, vol. 35, no. 5, Jul. 2023, doi: 10.1016/j.jksus.2023.102663.
35. S. Lal et al., "Antioxidant, antimicrobial, and photocatalytic activity of green synthesized ZnO-NPs from
36. Myrica esculenta fruits extract," Inorg Chem Commun, vol. 141, Jul. 2022, doi: 10.1016/j.inoche.2022.109518.
37. S. Irshad, M. Riaz, A. Anjum, S. Sana, R. Saleem, and A. Shaukat, "BIOSYNTHESIS OF ZnO NANOPARTICLES USING OCIMUM BASILICUM AND DETERMINATION OF ITS ANTIMICROBIAL ACTIVITY," J Anim Plant Sci, doi: 10.36899/japs.2020.1.0021.
38. H. Jan et al., "A detailed review on biosynthesis of platinum nanoparticles (PtNPs), their potential antimicrobial and biomedical applications," Journal of Saudi Chemical Society, vol. 25, no. 8, Aug. 2021, doi: 10.1016/J.JSCS.2021.101297.
39. J. J. Xu, W. C. Zhang, Y. W. Guo, X. Y. Chen, and Y. N. Zhang, "Metal nanoparticles as a promising technology in targeted cancer treatment," Drug Deliv, vol. 29, no. 1, pp. 664–678, 2022, doi: 10.1080/10717544.2022.2039804.
40. J. J. Xu, W. C. Zhang, Y. W. Guo, X. Y. Chen, and Y. N. Zhang, "Metal nanoparticles as a promising technology in targeted cancer treatment," Drug Deliv, vol. 29, no. 1, pp. 664–678, 2022, doi: 10.1080/10717544.2022.2039804.
41. J. Naik and M. David, "Phytofabrication of silver and zinc oxide nanoparticles using the fruit extract of Phyllanthus emblica and its potential anti-diabetic and anti-cancer activity," Particulate Science and Technology, vol. 41, no. 6, pp. 761–773, Aug. 2023, doi: 10.1080/02726351.2022.2141668.
42. K. K. Bharadwaj et al., "Green Synthesis of Gold Nanoparticles Using Plant Extracts as Beneficial Prospect for Cancer Theranostics," Molecules, 2021, doi: 10.3390/molecules26216389.
43. R. Geetha, T. Ashokkumar, S. Tamilselvan, K. Govindaraju, M. Sadiq, and G. Singaravelu, "Green synthesis of gold nanoparticles and their anticancer activity," Cancer Nanotechnol, vol. 4, no. 4–5, pp. 91–98, Aug. 2013, doi: 10.1007/s12645-013-0040-9.

44. S. N. Omer et al., "Molecular docking insights: interaction mechanisms of green-synthesized iron oxide nanoparticles with bacterial proteins," Microb Pathog, vol. 205, Aug. 2025, doi: 10.1016/j.micpath.2025.107704.
45. M. Kciuk et al., "Computational Bioprospecting Guggulsterone against ADP Ribose Phosphatase of SARS-CoV-2," Molecules, vol. 27, no. 23, Dec. 2022, doi: 10.3390/molecules27238287.
46. B. E. Sadoq et al., "Metal and Metal Oxide Nanoparticles: Computational Analysis of Their Interactions and Antibacterial Activities Against Pseudomonas aeruginosa," Bionanoscience, vol. 15, no. 1, Mar. 2025, doi: 10.1007/s12668-024-01625-4.
47. A. Mohammadpour et al., "Green synthesis, characterization, and application of Fe3O4 nanoparticles for methylene blue removal: RSM optimization, kinetic, isothermal studies, and molecular simulation," Environ Res, vol. 225, May 2023, doi: 10.1016/j.envres.2023.115507.
48. D. Rajan, R. Rajamanikandan, and M. Ilanchelian, "Investigating the biophysical interaction of serum albumins-gold nanorods using hybrid spectroscopic and computational approaches with the intent of enhancing cytotoxicity efficiency of targeted drug delivery," J Mol Liq, vol. 377, May 2023, doi: 10.1016/j.molliq.2023.121541.
49. S. Parveen, M. Ikram, A. Haider, I. Shahzadi, A. Ul-Hamid, and A. A. A. Hafez, "Optimized AgBr/PVPFe2O3 Nanostructures for Effective Catalytic and Biological Activities; Computational Insights," J Inorg Organomet Polym Mater, 2025, doi: 10.1007/s10904-025-03835-z.
50. M. Khatami, H. Q. Alijani, H. Heli, and I. Sharifi, "Rectangular shaped zinc oxide nanoparticles: Green synthesis by Stevia and its biomedical efficiency," Ceram Int, vol. 44, no. 13, pp. 15596–15602, Sep. 2018, doi: 10.1016/j.ceramint.2018.05.224.
51. K. Singh, J. Singh, and M. Rawat, "Green synthesis of zinc oxide nanoparticles using Punica Granatum leaf extract and its application towards photocatalytic degradation of Coomassie brilliant blue R-250 dye," SN Appl Sci, vol. 1, no. 6, Jun. 2019, doi: 10.1007/s42452-019-0610-5.
52. J. Chaudhary, V. Khoker, and G. Tailor, "SYNTHESIS AND CHARACTERIZATION OF ZINC NANOPARTICLES USING THERMOSETTING RESINS," Journal of Population Therapeutics and Clinical Pharmacology, Apr. 2024, doi: 10.53555/jptcp.v31i4.5374.
53. S. Akhter et al., "Cancer Targeted Metallic Nanoparticle: Targeting Overview, Recent Advancement and Toxicity Concern," 2011.
54. R. Geetha, T. Ashokkumar, S. Tamilselvan, K. Govindaraju, M. Sadiq, and G. Singaravelu, "Green synthesis of gold nanoparticles and their anticancer activity," Cancer Nanotechnol, vol. 4, no. 4–5, pp. 91–98, Aug. 2013, doi: 10.1007/s12645-013-0040-9.
55. J. Conde, G. Doria, and P. Baptista, "Noble Metal Nanoparticles Applications in Cancer," J Drug Deliv, vol. 2012, pp. 1–12, Oct. 2012, doi: 10.1155/2012/751075.
56. A. F. Burlec et al., "Current Overview of Metal Nanoparticles' Synthesis, Characterization, and Biomedical Applications, with a Focus on Silver and Gold Nanoparticles," Pharmaceuticals, vol. 16, no. 10, Oct. 2023, doi: 10.3390/PH16101410.
57. M. G. Heinemann, C. H. Rosa, G. R. Rosa, and D. Dias, "Biogenic synthesis of gold and silver nanoparticles used in environmental applications: A review," Trends in Environmental Analytical Chemistry, vol. 30, Jun. 2021, doi: 10.1016/J.TEAC.2021.E00129.
58. I. P. Omoregie et al., "Application of Mushrooms in the Bioremediation of Environmental Pollutants," in Mushroom Biotechnology for Improved Agriculture and Human Health, 2025, pp. 1–28. doi: https://doi.org/10.1002/9781394212699.ch1.
59. A. Kwatra et al., "Green ZnO nanoparticle synthesis using Tamarindus indica and application as a potent antibacterial and anticancer agent," Sustainable Chemistry for Climate Action, vol. 6, p. 100083, Jun. 2025, doi: 10.1016/J.SCCA.2025.100083.
60. R. Rajkumar, G. Ezhumalai, and M. Gnanadesigan, "A green approach for the synthesis of silver nanoparticles by Chlorella vulgaris and its application in photocatalytic dye degradation activity," Environ Technol Innov, vol. 21, Feb. 2021, doi: 10.1016/J.ETI.2020.101282.
61. L. Hernández-Morales et al., "Study of the green synthesis of silver nanoparticles using a natural extract of dark or white Salvia hispanica L. seeds and their antibacterial application," Appl Surf Sci, vol. 489, pp. 952–961, Sep. 2019, doi: 10.1016/j.apsusc.2019.06.031.
62. F. Zanjanchi, "Correction: A Computational Study on Iron Oxide Magnetite Nanoparticles As Adsorbents of Anionic Pollutants (Journal of Electronic Materials, (2022), 51, 5, (2178-2191), 10.1007/s11664-02209450-9)," May 01, 2022, Springer. doi: 10.1007/s11664-022-09541-7.

63. F. Zanjanchi, "A Computational Study on Iron Oxide Magnetite Nanoparticles As Adsorbents of Anionic Pollutants," J Electron Mater, vol. 51, no. 5, pp. 2178–2191, May 2022, doi: 10.1007/s11664-022-094509.
64. S. A. Mousa, D. A. Wissa, H. H. Hassan, A. A. Ebnalwaled, and S. A. Khairy, "Enhanced photocatalytic activity of green synthesized zinc oxide nanoparticles using low-cost plant extracts," Sci Rep, vol. 14, no. 1, Dec. 2024, doi: 10.1038/S41598-024-66975-1.

Tables

Table-1 : Dose-

	0 µg/mL	20 µg/mL	40 µg/mL	60 µg/mL	80 µg/mL	100 µg/mL	10 µg/mL (Streptomycin)
E. coli	++++	++++	+++	+++	+++	++	+
B. cereus	++++	++++	+++	++	++	+	+
S. aureus	++++	++++	+++	+++	++	++	+

Dependent antimicrobial Study of Nanoparticles

Table 2: Time-Dependent Antimicrobial Study of Nanoparticles Figures

	2 days	4 days	5 days	6 days	7 days
E. coli	++++	++++	+++	+++	++
B. cereus	++++	++++	+++	++	++
S. aureus	++++	++++	+++	+++	++